Available online at www.sciencedirect.com
ScienceDirect
Polymer 48 (2007) 1005–1011
polymer
www.elsevier.com/locate/polymer

# In vitro degradation and biocompatibility of poly(L-lactic acid)/chitosan fiber composites

Xiufang Zhang*, Hui Hua, Xinyuan Shen, Qing Yang

*College of Material Science and Engineering, State Key Laboratory for Modification of Chemical Fibers and Polymer Materials, Donghua University, 1882, West Yanan Road, Shanghai 200051, PR China*

Received 4 October 2006; received in revised form 12 December 2006; accepted 12 December 2006
Available online 20 December 2006

**Abstract**

In this study, poly(L-lactic acid) (PLLA) fibers were prepared by the dry–wet-spinning method, while chitosan (CHS) fibers were prepared via the wet-spinning method. The two fibers were blend spun and then fabricated into PLLA/CHS fabrics. In vitro degradation experiments of the fabrics were carried out in a phosphate-buffered solution at 37 °C with a pH of 7.4. Changes in molecular parameters (molecular weights and molecular weight distributions), phase structures (crystallinities), morphologies (fiber surface topologies) of the PLLA fibers, and their macroscopic properties (the fabric weight losses and mechanical strengths) were monitored with degradation times. These results were compared with control samples with no degradation. The hydrolysis mechanism of PLLA/CHS fabrics was analyzed. It was found that the degradation rate of dry–wet-spun PLLA fibers was higher than those of the melt-spun or dry-spun ones. Furthermore, the compatibility between PLLA/CHS fabrics and osteoblast under the in vitro degradation was investigated for the potential application of using the PLLA/CHS fabrics as supporting materials for chest walls and bones. Cell strain hFOB1.19 human SV40-transfected osteoblast and PLLA/CHS mixed fabrics were incubated. The cell morphology at early stages of cultivation was also studied. Excellent adhesion between osteoblast and PLLA/CHS fabrics was observed, indicating good biocompatibility of the fabrics with osteoblast.


*Keywords:* PLLA/CHS fabric; Dry–wet spinning; Osteoblast

## 1. Introduction

Poly(L-lactic acid) (PLLA) is an aliphatic polyester with good biodegradability, biocompatibility, reasonably good mechanical properties and processibility in forming fibers. In the past 40 years, PLLA has been extensively studied and utilized to be one type of the biomedical material in the areas of tissue engineering and drug delivery [1,2]. For practical applications of a biodegradable polymer material, it is important to understand rates and mechanisms of its biodegradation. It is generally considered that a simple hydrolysis is the main degradation mechanism for PLLA [3]. So far as reported, PLLA fibers for this purpose are obtained by either melt-spinning or dry-spinning method. The degradation rates of PLLA fibers prepared by these two methods are reported to be very slow, and thus its medical application as a biodegradable polymer is restricted. For example, Xiaoyan et al. studied the degradation of melt-spun PLLA fibers in a phosphate-buffered solution (PBS) with a pH of 7.4 at 37 °C. They found a substantial decrease in the molecular weight of PLLA, a minor decrease in tensile strength, and almost no change in the mass loss after 35 weeks. In addition, microcracks perpendicular to the fiber direction appeared after 45 weeks of degradation, indicating a decrease in the molecular weight of the PLLA fibers [4]. Joziasse et al. reported that a 25% loss in the mechanical properties of a dry-spun PLLA fiber can be observed after 5 years of degradation in PBS at room temperature under tension [5].

In this paper, we decided to pursue a preparation of PLLA fibers via a dry–wet-spinning method. A wet-spinning method

* Corresponding author. Tel.: +86 21 64459620; fax: +86 21 64455420.
*E-mail address:* xiufang@aol.com (X. Zhang).

0032-3861/$ - see front matter © 2006 Elsevier Ltd. All rights reserved.
doi:10.1016/j.polymer.2006.12.028

is used to prepare chitosan (CHS) fibers. Because the spinning processing conditions affect the structure and properties of the fibers, we expect that the degradation rates and mechanical properties of the dry–wet-spun PLLA fiber are also different [6–29]. Therefore, when the PLLA fibers are used as a part of an artificial chest wall, we may see different rates of degradation. In particular, we are interested in achieving faster degradation rates compared with PLLA fibers prepared by other methods. These changes may help to meet the requirements of the PLLA fibers for a medical device.

In order to achieve high biocompatibility with osteoblast and controllable degradation rates, PLLA fabrics and PLLA/CHS mixed fabrics were fabricated. In vitro degradation experiments in PBS with a pH value of 7.4 at 37 °C were carried out to evaluate the biodegradability of the PLLA/CHS fabrics. Under the chosen in vitro incubating conditions, the biocompatibility between PLLA/CHS mixed fabrics and osteoblast was tested. Potential applications of using the PLLA/CHS fabrics as supporting material for artificial chest walls and bones were explored. The cell morphology at early stages of cultivation was monitored, and the adhesion and biocompatibility between the osteoblast and PLLA/CHS mixed fabrics were evaluated.

## 2. Experimental section

### 2.1. Materials and sample preparations

PLLA pellets with an intrinsic viscosity of 2.67 dl/g were provided by the PURAC Company. Chitosan flakes were obtained from Dalian of China with a viscosity-average molecular weight of $4.5 \times 10^5$ g/mol and a deacetylation degree of 80%. Cell strain hFOB1.19 human SV40-transfected osteoblast was provided by the Shanghai Cell Institute of Chinese Science Academy. DMEM/F-12 culture medium containing 10% FBS and 0.3 mg/ml of G418 was provided by the GIBCO Company.

### 2.2. Fiber spinning and fabric processing

PLLA fibers were prepared via the dry–wet-spinning method. The PLLA pellets were dissolved in chloroform with storing first, and then the PLLA solution was put into a screw extruder at room temperature. The PLLA fibers were spun through a single nozzle spinneret (0.5 mm × 7 mm, *D*/*L*). The air gap between the spinneret and liquid bath was 5 cm (the dry stage of the spinning), and the coagulation bath solution was 100% alcohol with a bath temperature of 40–60 °C for the wet stage of spinning. At 135 °C, the PLLA fibers were drawn at different ratios in a silicone oil bath.

Chitosan pellets were dissolved in acetic acid at room temperature and the solution was then passed through a 500-nozzle spinneret with five layers of filter cloths to the coagulation bath. The coagulation bath solution was 10% sodium hydroxide and the bath temperature was 30 °C. Fibers were then washed by water at 40 °C and dried at room temperature.

PLLA fibers were first braided into a fabric slice with a size of 5 mm × 10 mm × 1 mm. These PLLA braids are denoted as references. The PLLA fiber and CHS fiber were braided into mixed fabric slices with a size of 5 mm × 10 mm × 1 mm, denoted as PLLA/CHS braids. These braids were sterilized by ethylene oxide and wetted by culture medium before cultivation with osteoblast.

### 2.3. Equipment and experiments

The weight losses of the PLLA fiber and PLLA/CHS braids were evaluated in a 7.4 pH PBS at 37 °C. The braid stripe, before degradation, was dried in vacuum and the weight was measured in a JY-B analytical balance. The stripe samples, during degradation, were first taken out of the degradation medium at different times and washed with de-ionized water. They were then dried in vacuum to eliminate all the residual medium liquids. These weights were then compared with the original sample weights before the degradation to calculate the percentage weight loss during the specific degradation time.

Molecular weight and molecular weight distribution changes in the PLLA fibers were evaluated in chloroform at 40 °C with a PL-GPC50 gel permeation chromatographer using two MIXED-B chromatographic columns with a polystyrene standard. The flow rate was 1 ml/min.

Crystallinity changes in the PLLA fibers during degradation were determined by two methods. The first method utilized differential scanning calorimetric (DSC) experiments via a Mettler-Toledo DSC-820. The DSC was calibrated following the standard procedure. The fibers were heated at rate of 10 °C/min under a nitrogen flow of 50 ml/min. The temperature range in the measurements was between 20 °C and 220 °C. The crystallinity data were calculated via the ratios between the measured heat of fusion and the equilibrium heat of fusion (93 J/g) [7].

The second method was using one-dimensional (1D) wide-angle X-ray diffraction (WAXD) experiments. The measurements were conducted on a Rigaku D/Meat-1200 X-ray diffractometer (Cu Kα). The X-ray was monochromatically filtered with a wavelength of 0.1541 nm. The diffraction angle ($2\theta$) range was between 6° and 30°. The calculation of the crystallinity via WAXD results followed the procedure of taking the ratio between the crystalline diffraction intensity and overall diffraction and scattering intensities (reference) after the air scattering was subtracted.

Based on the 1D WAXD pattern, the size of the crystallite grains were calculated based on the Scherrer equation:

$$L_{hkl} = \frac{k\lambda}{\beta \cos\theta} \tag{1}$$

where $L_{hkl}$ is the average dimension of the microcrystal vertical to the crystal face *hkl*, $k$ is the Scherrer shape-dependent constant (a value of 0.9 is adopted here), $\lambda$ is the wavelength of the incident X-ray (in nm), and $\beta$ is the half-width of the diffracted rays (in radians).

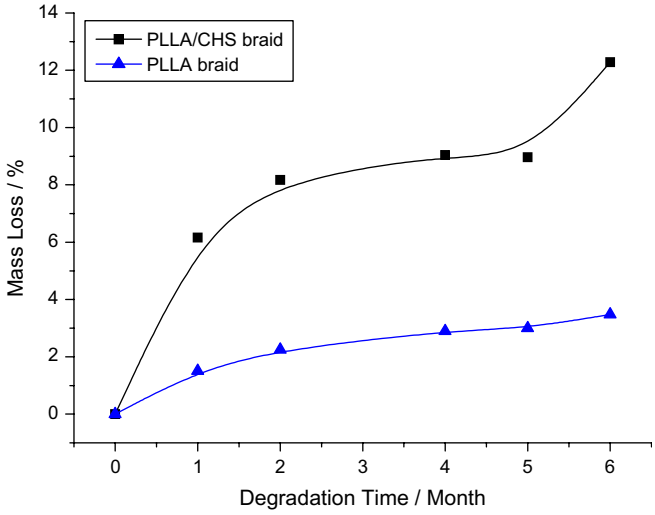


Fig. 1. Mass loss of PLLA/CHS braid and PLLA braid during degradation in pH 7.4 phosphate-buffered solution at 37 °C.

The surface morphological characterization of the original and cultivated PLLA fibers, the PLLA braid, and the PLLA/CHS braid sample at different degradation stages were studied with JSM-5600LV scanning electron microscopy (SEM). The samples were first dried and sputter-coated with gold in vacuum. The SEM voltage was 20 kV.

A DXLL-20000 universal testing machine was utilized to measure the tensile properties of the PLLA and PLLA/CHS braids at room temperature. The sample length was controlled to be 10 mm and the drawing rate was 20 mm/min.

The hydrolysis of the PLLA and PLLA/CHS braids (5 mm × 10 mm × 1 mm) was performed in a glass bottle with 30 ml phosphate-buffered solution (pH = 7.4 ± 0.1). The soaking temperature was 37 °C. The degradation system was kept static and was sampled monthly (a sample was taken out of the degradation medium and washed with de-ionized water). They were then dried in vacuum.

Cultivation was assisted by the Shanghai Biomaterial Testing Center. The sample was soaked fully in the culture medium and placed on the 24-hole cell cultivation plate with 1 piece of sample per hole. After a period of time, an osteoblast suspension with a cell concentration of $1 \times 10^6$/ml was gently placed on the sample surface. They were then cultivated in a 5% $CO_2$ culture box at 37 °C and saturated humidity followed by fixture with glutaraldehyde.

## 3. Results and discussion

### *3.1. Changes in molecular characteristics of the PLLA fiber braids*

Fig. 1 shows two sets of mass loss data for melt-spun PLLA fibers and dry–wet-spun PLLA fiber braids under the conditions of a 7.4 pH phosphate-buffered solution at 37 °C. Compared with the mass loss of the melt-spun PLLA fiber braids, the dry–wet-spun PLLA fiber braids exhibit larger mass loss at the same degradation time. The slopes of the mass loss curves in Fig. 1 represent speed of the degradation. More interestingly, it is evident that for the melt-spun PLLA fiber braids, the speed of degradation gradually decreases with increasing time; while, the three steps of the degradation process can be recognized from the mass loss of dry–wet-spun PLLA fiber braids. The initial fast degradation is the first step within the first month. Then, the speed decreases and keeps almost constant in between month 1 and month 5. After the 5-month period, the third step shows that the speed of degradation increases again. These distinct degradation kinetics between the melt-spun and the dry–wet-spun PLLA fibers reflect different structures and morphologies of the fibers prepared by theses two spinning methods (see below).

Fig. 2 shows GPC results of the PLLA fiber samples after they were separated and taken from the PLLA braid and the PLLA/CHS braid after 0, 2, 4, and 6 months of the hydrolysis degradation. It can be seen that as degradation continued,

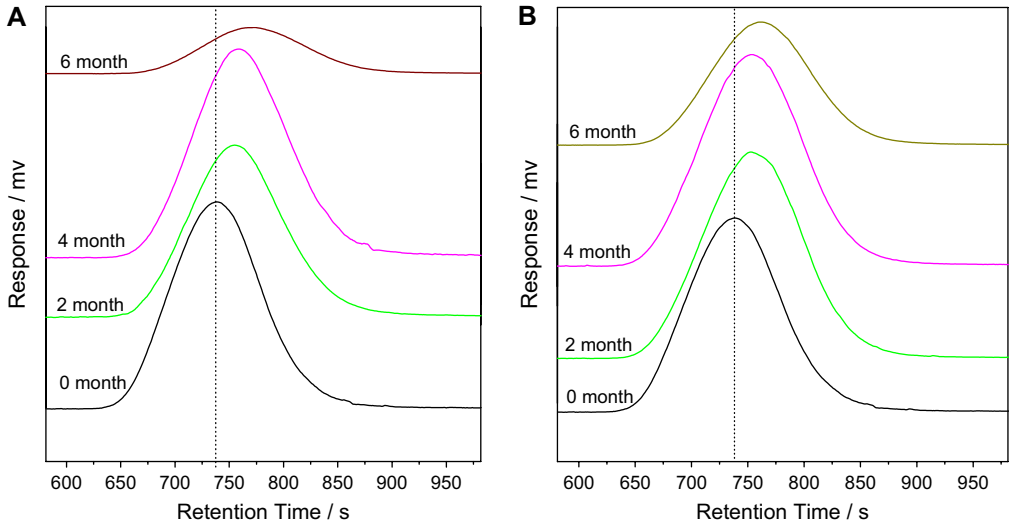


Fig. 2. GPC results of PLLA fiber from (A) PLLA braid and (B) PLLA/CHS braid at different hydrolysis times.

Table 1
GPC values of PLLA fibers of braid during degradation in pH 7.4 phosphate-buffered solution at 37 °C

| Degradation time (month) | PLLA/CHS braid | | PLLA braid | |
|---|---|---|---|---|
| | $M_n \times 10^5$ (g/mol) | $M_w/M_n$ | $M_n \times 10^5$ (g/mol) | $M_w/M_n$ |
| 0 | 7.5 | 1.59 | 7.5 | 1.59 |
| 2 | 6.1 | 1.76 | 6.0 | 1.71 |
| 4 | 6.1 | 1.70 | 5.7 | 1.68 |
| 6 | 5.2 | 1.85 | 3.1 | 2.01 |

retention time of the sample slowly shifts to the right, that is, the molecular weight decreases. In addition, after 6 months of degradation, the molecular weight distribution becomes broader, which is also confirmed by the data listed in Table 1.

Table 1 lists the changes in molecular weights of the PLLA fibers with the degradation time. It is evident that the molecular weight decreases continuously with an increase in the degradation time. After 6 months of degradation, the molecular weight loss of the PLLA fiber taken out of the PLLA braid was larger than that of the PLLA/CHS braid. The molecular weight loss of PLLA in each of the braids is 58% and 37%, respectively, indicating that the PLLA fibers in the PLLA braids are degraded slightly faster than those in the PLLA/CHS braids. The reason may be that the carboxyl groups produced by the hydrolysis of PLLA fibers promoted its degradation; while, the aminoglucose produced by hydrolysis in the PLLA/CHS braid neutralized the acidic degradation products and thus inhibited the degradation of PLLA fiber. Comparing Fig. 1 with Table 1, one can see that the changes in the molecular weights and the masses are not synchronous. This can be understood because the breakage of the ester bonds during degradation leads to the formation of low molecular weight products, and thus molecular weight decreases continuously and the molecular weight distribution becomes increasingly broader. On the other hand, during degradation only a small portion of the degraded macromolecular fragments will become small enough to be soluble in the phosphate-buffered solution, and therefore the mass losses lag behind the molecular weight decreases.

### 3.2. Changes in PLLA structure and morphology during degradation

Both DSC and WAXD experiments are used to determine the crystalline structure of PLLA fibers. The results are shown in Fig. 3A and B, respectively. The PLLA degradation is first carried out through hydrolysis of the amorphous PLLA. After this hydrolysis is almost completed, hydrolysis in the crystalline area then begins to take place due to the continuous penetration of water molecules [8]. Table 2 lists the crystallinities, crystallite sizes, and melt temperatures of the PLLA fibers in two braids before and after 6 months of degradation. After 6 months of degradation, the crystallinities of the PLLA fiber in both the PLLA braid and the PLLA/CHS braid are decreased; while, there is no change in the melting temperatures. The decrease in the crystallinity indicates that the hydrolysis in the amorphous area was complete and began to occur in the crystalline area. The decreasing degree of crystallinity further confirmed the inhibition of chitosan fibers on the hydrolysis of PLLA fiber.

It can also be found in Table 2 that after 6 months of degradation, the absolute values of the crystallinities of the PLLA fiber measured by DSC and WAXD are different. This was mainly due to the fact that the equilibrium heat of fusion we used, 93 J/g, may be still lower than the true equilibrium heat of fusion and/or the $2\theta$ angle region scanned in our experiments was limited [9]. The decrease in the crystallinity measured by DSC and WAXD experiments and the decrease in the crystallite sizes vertical to the crystal face ($L_{110}$) measured by WAXD experiments (see Table 2) indicate that the hydrolysis in the amorphous area has been completed and the hydrolysis in the crystalline area begins to occur.

Fig. 4a and b shows SEM micrographs of the PLLA fiber surface obtained by melt spinning and dry–wet spinning,

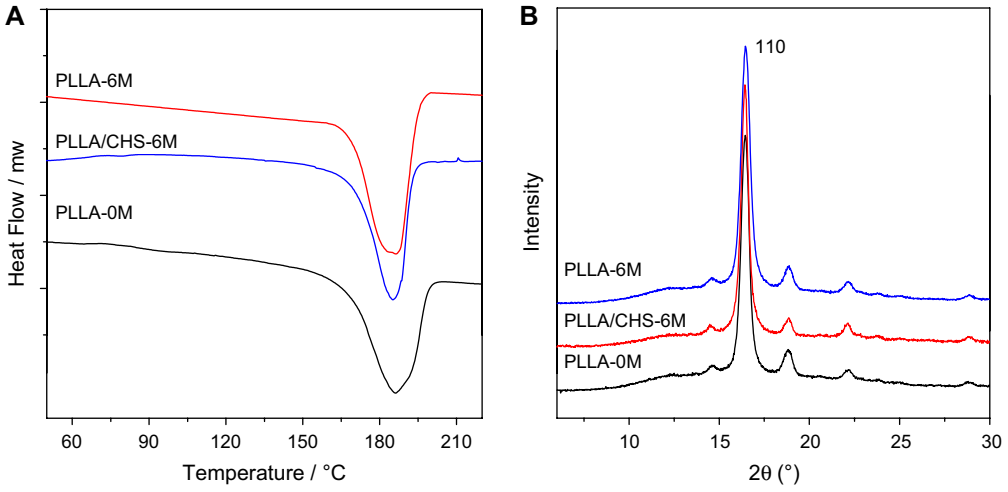


Fig. 3. Crystallinity changes during degradation: (A) DSC thermogram and (B) XRD diagram of PLLA fibers of braid during degradation in pH 7.4 phosphate-buffered solution at 37 °C.

Table 2
Crystalline properties of PLLA fiber before and after hydrolysis for 6 months

| Sample | $\Delta H_m$ (J/g) | $\beta$ (°) | $L_{110}$ (nm) | $X_{c,h}$ (%) | $X_{c,x}$ (%) | $T_m$ (°C) |
|---|---|---|---|---|---|---|
| PLLA-0M | 45.2 | 0.52 | 30.7 | 48.6 | 67.2 | 185.9 |
| PLLA-6M | 35.1 | 0.60 | 26.6 | 37.7 | 59.1 | 185.0 |
| PLLA/CHS-6M | 39.1 | 0.50 | 28.9 | 42.1 | 62.3 | 186.2 |

$X_{c,h}$: crystallization measured by DSC; $X_{c,x}$: crystallization measured by XRD; PLLA-0M: original PLLA fiber; PLLA-6M: PLLA fiber from PLLA braid after 6 months; PLLA/CHS-6M: PLLA fiber from PLLA/CHS braid after 6 months.

respectively. In fibers via the melt spinning, no microholes exist on the fiber surface. The crystal structure becomes more compact after fiber drawing. Therefore, it is more preventative for water attack of the fiber. While in the fibers formed via dry–wet spinning, a lot of microholes exist on the fiber surface, which is coarse, and its crystal structure is loose and incomplete. As a result, water molecules can easily enter into the fiber. The formation of this type of fiber surface is due to the fact that a double diffusion process occurs during the fiber spinning. Namely, the solvent diffused from the spinning dope into the coagulation bath accompanied by the diffusion of the precipitant from the coagulation bath into the spinning dope. After water gets into the fibers, it hydrolyzes the amorphous areas and leaves the crystalline parts to be dropped off from the fibers, and leads to an increase in the mass loss. This is proven by the experimental observation that after hydrolysis for 2 months, many insoluble, small grains were observed to suspend in the degradation medium when shaking the glass bottle containing the braid. As the degradation time increased, water molecules continue to enter into the fibers and hydrolyze the crystalline area of the PLLA fibers.

Fig. 5a is an SEM micrograph of a PLLA fiber before degradation and Fig. 5b is an SEM micrograph of a PLLA fiber taken from the PLLA/CHS braids after 6 months of degradation. Fig. 5c and d is SEM micrographs of PLLA fibers taken from the PLLA braid after 6 months of degradation. After 6 months of degradation, large cracks along the groove direction appeared on the fiber surfaces and traces of partial material falling off can be observed. Comparing Fig. 5b with Fig. 5d, one can see that cracks on the surface of the PLLA fiber taken from the PLLA braid are larger than those from the PLLA/CHS braid, but the surface of the PLLA fiber from the PLLA/CHS braid is coarser. It is known that the surfaces of PLLA fibers are susceptible to corrosive degradation in an alkalescent environment. The alkaline product of chitosan degradation would inhibit the hydrolysis of PLLA; while, the local alkaline microenvironment it created at the PLLA/CHS interfaces would erode the surfaces of the PLLA fibers and make the fiber surfaces coarser. Cracks were first caused by the breaking of the weak intermolecular van der Waals force and hydrogen bonding in the transversal direction of the fibers. After that, since the inter-macromolecular interactions were weakened with the time of in vitro degradation, the cracks expand continuously and penetrate into the inside of the fibers. Consequently, the material's tensile properties decrease.

### 3.3. Changes in mechanical properties of the PLLA fibers during degradation

The change in the breaking force of the two braids with degradation time is illustrated in Fig. 6. It can be found that before degradation, the breaking force of the PLLA/CHS braid is larger than that of the PLLA braid; while, after 1 month of degradation, they become opposite. The breaking force of the PLLA braid decreases with an increase in the degradation time and reaches 35% after 6 months of degradation. The molecular weight and entanglements of the chains certainly affect the mechanical properties of the polymer greatly [6]. During the hydrolysis of PLLA, both the molecular weight and the number of entangled chains decreases, causing a decrease in the breaking force of the braid. That is, the mechanical properties become poor after degradation.

### 3.4. Morphology of cell-supporting material complex

It can be seen that there are cells adhering to the surface of the PLLA/CHS braid after 2 days of cultivation with osteoblast (Fig. 7b). The shapes of the cells are flat, rhombic and polygonal. The survival of the cells was good.

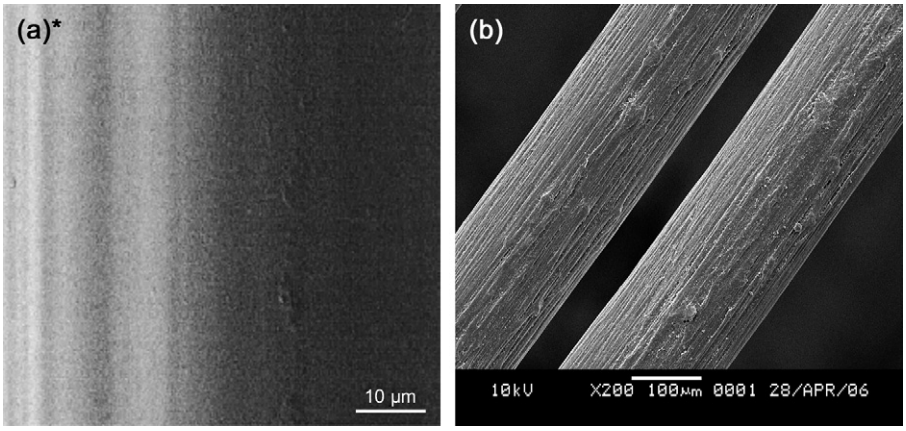


Fig. 4. SEM micrographs of the PLLA fibers obtained from (a, ×3000) melt spinning and (b, ×200) dry–wet spinning. (*) Reference from the literature of Xiaoyan et al. [4].

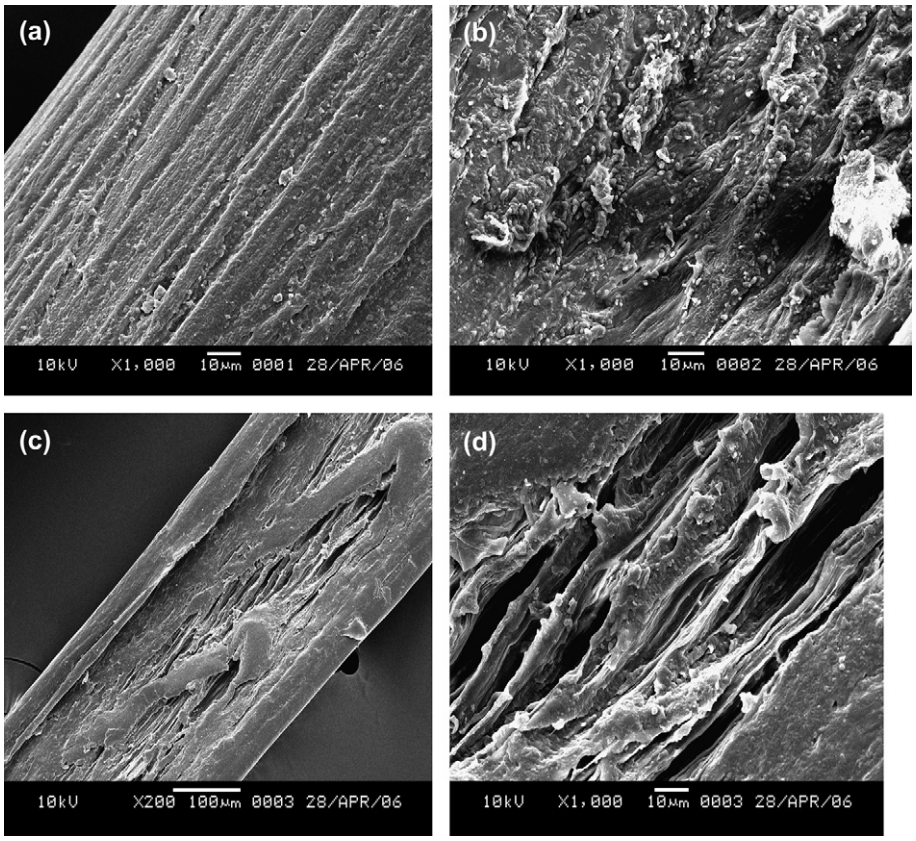


Fig. 5. Set of SEM micrographs of PLLA fiber from PLLA/CHS braid and PLLA braid at different hydrolysis times: (a) original PLLA fiber (×1000); (b) PLLA fiber from PLLA braid after hydrolysis at 37 °C for 6 months (×1000); (c) PLLA fiber from PLLA/CHS braid after hydrolysis at 37 °C for 5 months (×200); (d) is a magnification of (c) ×1000.

There are several advantages in using the PLLA/CHS fabric material. First, the elasticity of the material, vertically and horizontally, is good and the permeable pore-structure, characteristic of meshed braids, provides rooms for the cells and tissue regeneration. Secondly, the local inflammation and excessive acidity caused by PLLA hydrolysis were reduced, as the alkalescent free $NH^{2+}$ from chitosan hydrolysis can neutralize the acidic PLLA degradation products. Thirdly, chitosan introduced OH and $NH^{2+}$ polar groups into the material surface and thus improved its hydrophilicity and affinity to the cells. It makes osteoblast to distribute evenly on the braid net, increasing its compatibility with the tissues and the bonding forces between the braid net and the tissue cells. In addition, chitosan can also attract macrophage and promote the growth of platelets and blood vessels. All these favor the growth of blood vessels from the surface to the inside of the fiber and the formation of the three-dimensional substance of bone.

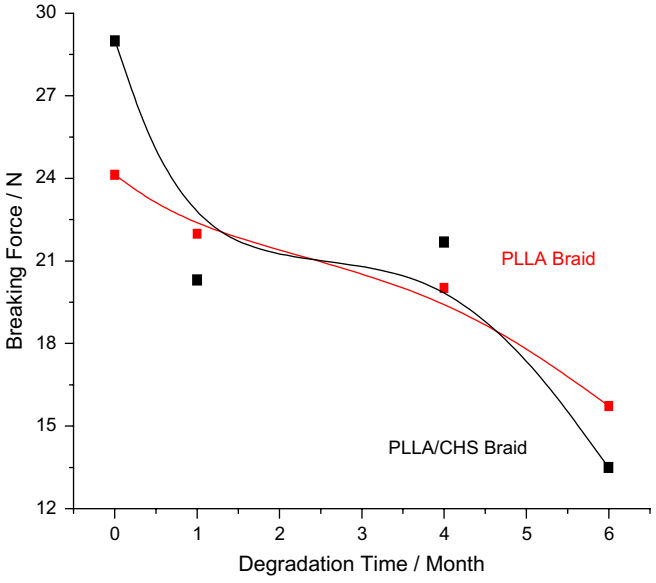


Fig. 6. The changes in the breaking force of PLLA braid and PLLA/CHS braid at different periods of degradation in vitro.

## 4. Conclusion

Through the analysis of the results of in vitro degradation of the PLLA braid, it has been found that compared with melt-spun and dry-spun fibers, there is an obvious increase in the degradation rate of dry–wet-spun PLLA fibers in the phosphate-buffered solution. Therefore, the biodegradation rate of PLLA fibers can be adjusted by changing the spinning process thus meeting the requirements of other uses. In other words, the biodegradation and the mechanical properties of dry–wet-spun PLLA fibers depend highly on the fiber-formation process since the spinning process determines the fibers'

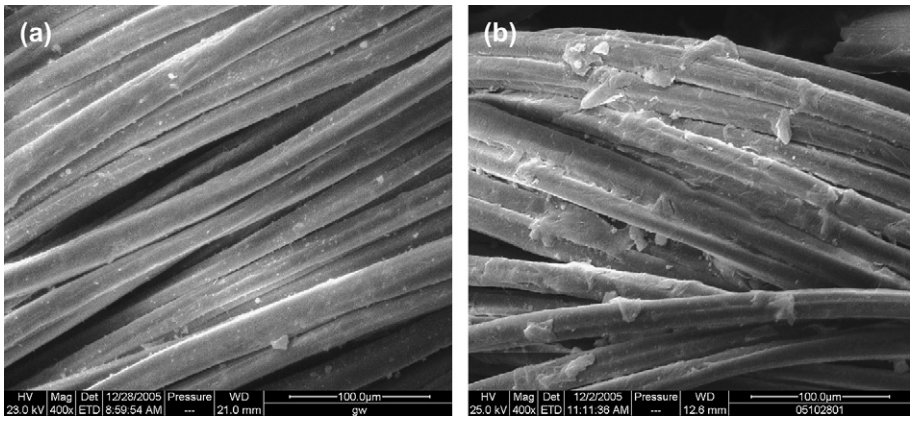


Fig. 7. SEM micrograph of blank sample (a) and PLLA/CHS braid–osteoblast complex (b) after 2 days of cultivation.

chemical–physical structure and the physical properties. The PLLA/CHS braid prepared from dry–wet-spun PLLA fibers and wet-spun chitosan fibers may be a probable candidate as an ideal osteoblast carrier for the repairing of damaged chest wall and bones in a large area. It can also be an ideal cell carrier for tissue engineering since the pore-size and porosity of the PLLA/CHS braid can be adjusted according to the cell characteristics.

## Acknowledgements

We thank Prof. Zhifei Xu and Mr. Bailin Gu for supporting this project. We thank also Prof. Jiao Sun for contribution to the biocompatibility measurement of the osteoblast.

## References

[1] Doi Y, Steinbuchel A, Chen G-Q. Polyesters III: applications and commercial products. In: Biopolymers, vol. 4. Beijing: Chemical Industry Press; 2004. p. 152–3.
[2] Zhang Z-Y, Yan Y-H. Fine Specialty Chem 2005;13(14):7–19 [in Chinese].
[3] Pegoretti A, Fambri L, Migliaresi C. J Appl Polym Sci 1997;64: 213–23.
[4] Xiaoyan Y, Arthur FTM, Kangde Y. J Appl Polym Sci 2002;85: 936–43.
[5] Joziasse CAP, Grijpma DW, Bergsma JE. Colloid Polym Sci 1998; 276(11):276–968.
[6] Ikada Y, Tsuji H. Macromol Rapid Commun 2000;21:117.
[7] Tsuji H, Ikada Y. Polylactides. Kyoto: Koubunshi Kankoukai Inc.; 1997.
[8] Shimamoto T, Oka T, Adachi M, Hyon SH, Nakayama K, Kaito A. US Patent 54-31652 [to Gunze Co. Ltd.]; 1995.
[9] Perego G, Cella GD, Bastioli C. J Appl Polym Sci 1996;59:37.
[10] Tadokoro H. Structure of polymers. Kyoto: Kagaku Dojin; 1976.
[11] Pranamuda H, Tokiwa Y, Tanaka H. Appl Environ Microbiol 1995; 61:1828.
[12] Fambli L, Prgoretti A, Fenner R, Incardona SD, Migliaresi C. Polymer 1997;38:79.
[13] Okuzaki H, Kubota I, Kunugi T. J Polym Sci Part B 1999;37:991.
[14] Hyon SH, Jamshidi K, Ikada Y. Polymers as biomaterials. In: ACS symposium series. New York: Plenum Press; 1984. p. 51–65.
[15] Eling B, Gogolewski G, Pennings AJ. Polymer 1982;23:1587.
[16] DeSantis P, Kovacs AJ. Biopolymers 1968;6:299.
[17] Kalb B, Pennings AJ. Polymer 1980;21:607.
[18] Hoogsteen W, Postema AR, Pennings AJ, Brinke GT, Zugenmaier P. Macromolecules 1990;23:634.
[19] Kobayashi J, Asahi T, Ichikawa M, Oikawa A, Suzuki H, Watamabe T, et al. J Appl Phys 1995;77:2957.
[20] Miyata T, Masuko T. Polymer 1997;38:4003.
[21] Puiggali J, Ikada Y, Ysuji H, Cartier L, Okihara T, Lotz B. Polymer 2000;41:8921.
[22] Leenslag JW, Pennings AJ. Polymer 1987;28:1695.
[23] Sawai D, Takahashi K, Imamura T, Nakamura K, Kanamoto T, Hyon SH. J Polym Sci Polym Phys Ed 2002;40:95.
[24] Griswold PD, Zachariades AE, Porter RS. Polym Eng Sci 1978; 18:861.
[25] Cohn D, Younes H. J Biomed Mater Res 1988;22:993.
[26] Lee JK, Lee KH, Jin BS. Eur Polym J 2001;37:907.
[27] Kang S, Hsu SL, Stidham HD, Smith PB, Leugers MA, Yang X. Macromolecules 2001;34:4542.
[28] Monnerie L. In: Ward IM, editor. Developments in oriented polymers-2. London: Elsevier Applied Science; 1987 [chapter 6].
[29] Kellogg GJ, Walton DG, Mayes AM, Lambooy P, Russell TP, Gallagher PD, et al. Phys Rev Lett 1996;76:2503.